

ECoLAD: Deployment-Oriented Evaluation for Automotive Time-Series Anomaly Detection

Kadir-Kaan Özer^{1,2}, René Ebeling¹, MarkusENZweiler²

Abstract—Time-series anomaly detectors are commonly compared on workstation-class hardware under unconstrained execution. In-vehicle monitoring, however, requires predictable latency and stable behavior under limited CPU parallelism. Accuracy-only leaderboards can therefore misrepresent which methods remain feasible under deployment-relevant constraints.

We present *ECoLAD* (Efficiency Compute Ladder for Anomaly Detection), a deployment-oriented *evaluation protocol* instantiated as an empirical study on proprietary automotive telemetry (anomaly rate ≈ 0.022) and complementary public benchmarks. *ECoLAD* applies a monotone compute-reduction ladder across heterogeneous detector families using mechanically determined, integer-only scaling rules and explicit CPU thread caps, while logging every applied configuration change. Throughput-constrained behavior is characterized by sweeping target scoring rates and reporting (i) coverage (the fraction of entities meeting the target) and (ii) the best AUC-PR achievable among measured ladder configurations satisfying the target. On constrained automotive telemetry, lightweight classical detectors sustain both coverage and detection lift above the random baseline across the full throughput sweep. Several deep methods lose feasibility before they lose accuracy.

I. INTRODUCTION

Modern intelligent vehicles continuously produce telemetry from powertrain, chassis, electronic control units (ECUs), and body controllers. Detecting abnormal patterns in these signals supports early fault discovery, predictive maintenance, and safety monitoring. We treat onboard monitoring as the primary deployment use case, where latency must be predictable and CPU parallelism is severely limited. Fleet backend analytics represents a secondary application context. In either setting, detection quality alone is insufficient: inference latency must be predictable, resource usage must fit system limits, and score behavior must remain stable enough to support threshold calibration on nominal data.

Many TSAD (time-series anomaly detection) studies optimize and compare detection quality under unconstrained execution. Embedded deployment imposes two coupled stresses: reduced compute budgets and reduced CPU parallelism (often near single-threaded execution). Under these constraints, method rankings can drift and feasibility can be dominated by runtime overheads (data movement, preprocessing, framework setup) that are invisible on accelerated backends.

This paper introduces *ECoLAD*, a deployment-oriented evaluation *protocol* that (i) reduces compute monotonically across tiers, (ii) caps CPU parallelism explicitly, and (iii) characterizes throughput-constrained behavior via a sweep of

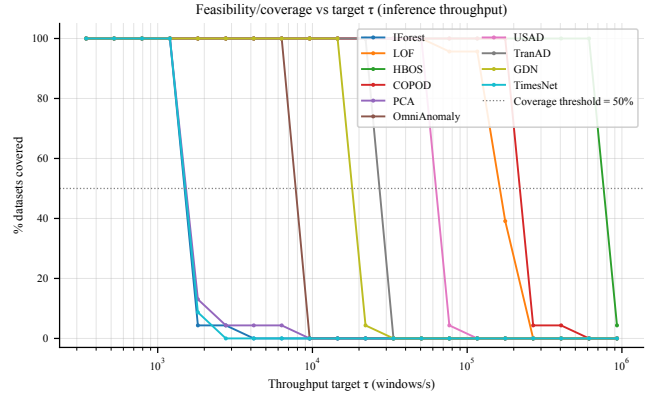


Fig. 1: Throughput feasibility CDF under a fixed tier. Each curve shows the fraction of evaluated entities whose throughput exceeds a target threshold τ , computed as $wps = N/t_{inf}$ (Sec. III-G). The horizontal line marks the 50% feasibility reference.

throughput targets τ , reporting coverage and mean achievable AUC-PR under the constraint. Fig. 1 provides a feasibility overview.

We study three research questions: (RQ1) how detection metrics and model ranking change when moving from a high-performance reference configuration to constrained tiers; (RQ2) which detector families degrade gracefully under systematic compute reduction versus failing sharply due to architectural or implementation bottlenecks; and (RQ3) on the constrained (CPU-1T) tier, how coverage and mean achievable AUC-PR change as τ increases.

Our contributions are threefold. First, we specify an auditable compute ladder with explicit tier definitions, thread caps, mechanically determined integer-only scaling rules, and per-run configuration diffs. Table I positions *ECoLAD* against representative prior evaluation resources. Second, we report detection quality jointly with runtime and throughput across tiers, including tier-wise Pareto analysis. Third, we provide a reproducible operating-point selection mechanism for throughput constraints that supports target sweeps without label-dependent retuning on evaluation data.

II. RELATED WORK

Benchmarking and evaluation practice in TSAD is sensitive to metric choices, labeling semantics, and pipeline details. TimeEval provides a benchmarking toolkit and standardized execution environment [2]. Schmidl et al. present a comprehensive empirical evaluation and discuss how algorithm rankings depend on evaluation choices [1]. Zhang et al. analyze effectiveness and robustness across algorithm classes

¹Mercedes-Benz AG, Germany. {kadir.oezer, rene.ebeling}@mercedes-benz.com

²Institute for Intelligent Systems, Esslingen University of Applied Sciences, Germany. markus.enzweiler@hs-esslingen.de

TABLE I: Comparison of representative TSAD evaluation resources. ✓ = explicitly operationalized; ● = partial/proxy; ✗ = not addressed. RT: runtime/latency measured or enforced; Range: range-aware evaluation; VUS: VUS (volume under the surface) metrics; Ladder: explicit monotone multi-tier compute ladder; Threads: explicit CPU parallelism cap; Match: throughput/feasibility matching; Trade: explicit quality–cost analysis; Audit: structured reporting of config/failures; Toolkit: reusable pipeline; Public: public artifacts; Online: online leaderboard; Auto: automotive/ECU context.

Work	Type	RT	Range	VUS	Ladder	Threads	Match	Trade	Audit	Toolkit	Public	Online	Auto
ECoLAD (this work)	Protocol + empirical eval.	✓	✗	✗	✓	✓	✓	✓	✓	●	✗	✗	✓
Schmidl et al. [1]	Empirical evaluation	✓	✓	✗	✗	✓	✗	✓	✓	●	●	✗	✗
Wenig et al. (TimeEval) [2]	Toolkit	✓	✓	✗	✗	●	✗	●	✓	✓	✓	✗	✗
Zhang et al. [3]	Empirical evaluation	✓	✓	✗	✗	✗	✗	✓	●	●	✓	✗	✗
Qiu et al. (TAB) [4]	Benchmark + pipeline + leaderboard	✓	✓	✓	✗	✗	✗	✓	✓	✓	✓	✓	✗
Si et al. (TimeSeriesBench) [5]	Benchmark + toolkit + leaderboard	✓	✓	✗	✗	✗	✗	✓	●	✓	✓	✓	✗
Lavin & Ahmad (NAB) [6]	Benchmark	✗	✓	✗	✗	✗	✗	✗	●	✓	✓	●	✗
Choudhary et al. [7]	Empirical eval./guide	✓	✗	✗	✗	✗	✗	✓	✗	✗	✗	✗	✗

and both point and range metrics [3]. Recent initiatives aim to unify TSAD benchmarking suites and leaderboards, including TAB [4] and TimeSeriesBench [5]. NAB incorporates latency-aware benchmarking semantics for real-time detection [6]. Runtime–efficacy trade-offs for streaming detection have been emphasized as an evaluation requirement [7].

ECoLAD differs in emphasis: it treats *compute reduction* and *CPU parallelism caps* as first-class protocol variables, and formalizes throughput-target analysis under constrained execution as a reproducible, auditable procedure. Where prior efforts primarily standardize datasets, metrics, and execution environments, ECoLAD standardizes how model capacity and parallelism are *reduced* and how feasibility under a target scoring rate is determined.

III. ECoLAD PROTOCOL AND STUDY DESIGN

A. Protocol Scope

ECoLAD is a reusable evaluation protocol defined by: (i) fixed scoring semantics (windowing and metric computation), (ii) a monotone compute-reduction ladder (tiered scaling rules), (iii) explicit CPU thread caps per tier, and (iv) auditable logging of configuration diffs and profiling outputs (see Table II). The CPU–1T tier isolates the effect of single-thread execution as a conservative stress test for reduced parallelism. Here, we do not use a cycle-accurate ECU emulator. Therefore, a platform-specific correction factor should be applied when mapping the reported throughput numbers to a specific target microarchitecture.

B. Datasets and Splits

Proprietary vehicle measurement dataset (Telemetry). The primary dataset is a proprietary in-vehicle measurement time series with 80,000 datapoints and 19 synchronized features. We use a contiguous split: 40,000 datapoints for training (20% held out as validation, 32,000 as training proper) and 40,000 for testing. Anomaly labels are derived from synchronized fault event logs recorded by the vehicle’s diagnostic system. They mark contiguous intervals of confirmed abnormal operation. The labeled anomaly rate is 0.02184, implying a random-scorer AUC-PR baseline of 0.022. Labels are used only for evaluation and feasibility statistics. The feature set comprises synchronized powertrain

inverter/coordinator signals, steering and chassis kinematics, wheel/brake measurements, and vehicle motion channels (speed, acceleration, yaw). As Telemetry is a single long recording, distributional throughput statistics (p10/p90) are drawn primarily from SMD and SMAP.

SMD (Server Machine Dataset). For RQ2 we additionally use SMD, a widely used public TSAD benchmark of multivariate server monitoring metrics with labeled anomalies across multiple machines (introduced in the context of OmniAnomaly [8]). SMD comprises 22 entities and stresses robustness under heterogeneous dynamics and different anomaly manifestations than vehicle telemetry.

SMAP (Soil Moisture Active Passive). For throughput-target feasibility experiments (RQ3) we include SMAP [9], a public benchmark of multivariate spacecraft telemetry streams with labeled anomalies.

Seeds. All reported results are aggregated over two random seeds. For deterministic classical methods (HBOS, COPOD, LOF, IForest, PCA) seeds have no effect. Seed-to-seed AUC-PR standard deviations for the five neural methods ranged from 0.000 to 0.003 across all tiers, confirming two seeds are sufficient to characterize mean behavior at the precision reported in the results tables.

C. Execution Environment and Measurement Protocol

All experiments were run on an Apple MacBook Pro with an M3 Max CPU/GPU and 32 GB of unified memory. Thread caps were enforced via PyTorch `set_num_threads / set_num_interop_threads`, `OMP_NUM_THREADS`, and BLAS thread limits were set before each run. All caps are logged per run as part of the audit schema. The M3 Max exposes 14 performance cores. CPU–MT uses all 14, CPU–LT uses 7, and CPU–1T uses 1. For each (method, tier, entity), runtime is measured as synchronized wall time around the full execution (`total_time_s`). When an implementation exposes phase timings, we additionally record training time (`fit_time_s`) and inference-only scoring time (`infer_time_s`). Training time is treated as an offline diagnostic rather than a deployment cost proxy.

D. Benchmark/Evaluation Comparison Matrix

Table I positions ECoLAD relative to representative TSAD evaluation resources using strict, evidence-aligned semantics:

TABLE II: Tier definitions: backend, thread cap, and compute-reduction factor s . CPU-1T is the primary deployment-stress tier.

Tier ID	Backend	Thread cap	Scale s
GPU	GPU (M3 Max)	uncapped (14)	1.00
CPU-MT	CPU multi-thread	14	0.75
CPU-LT	CPU limited-thread	7	0.50
CPU-1T	CPU single-thread	1	0.25

✓ only if a feature is explicitly operationalized; ● for partial/proxy support; ✗ if not addressed.

E. Budget Tiers: Device, Threads, Work Scale

We use four tiers (Table II), each specifying (i) the execution backend (accelerated vs. CPU), (ii) an explicit CPU thread cap, and (iii) a compute-reduction factor $s \in \{1.0, 0.75, 0.50, 0.25\}$ that mechanically reduces model and training workload according to Sec. III-F. For methods without GPU-accelerated implementations (all five classical detectors), the GPU tier reduces to the reference configuration on CPU. Only the thread cap and scale semantics differ across tiers for those methods.

F. Mechanical Hyperparameter Scaling

For each method, a baseline configuration is transformed mechanically by tier scaling rules. Scaling is integer-only and monotone. No per-tier retuning is performed. Let s denote the tier compute-reduction factor. Integer hyperparameters are grouped by role and scaled as:

$$v'_{\text{work}} = \max(1, \text{round}(s v)), \quad (1)$$

$$v'_{\text{width}} = \max(1, \text{round}(\sqrt{s} v)), \quad (2)$$

$$v'_{\text{heads}} = \max(1, \text{round}(\sqrt{s} v)), \quad (3)$$

$$v'_{\text{depth}} = \max(1, \text{round}(s^{1/4} v)), \quad (4)$$

$$v'_{\text{window}} = \max(8, \text{round}(\sqrt{s} v)). \quad (5)$$

If scaling creates invalid combinations (e.g., embedding size not divisible by attention heads), a conservative constraint-repair step minimally adjusts affected dimensions. Exponents are chosen so compute decreases roughly proportionally with s while avoiding degenerate architectures: width and heads scale with \sqrt{s} (capacity scales quadratically with width, so \sqrt{s} halves capacity when $s = 0.25$); depth scales with $s^{1/4}$ to avoid collapsing shallow models too aggressively at low s . Repairs were required in fewer than 4% of runs, affecting only attention-head/embedding-size alignment in TranAD and GDN at the CPU-LT and CPU-1T tiers. Parameters that change decision semantics (e.g., contamination/threshold-like controls) are intentionally not scaled. Continuous hyperparameters follow baseline implementations, which commonly use Adam [10].

G. System Proxies and Cost Normalization

a) Timing definitions: We distinguish between inference-only time (\tilde{t}_{inf}) and full-run time (t_{e2e}) to avoid conflating offline training overhead with online scoring capacity. This distinction is critical for methods such as OmniAnomaly,

TABLE III: Evaluated detectors and references.

Method	Reference
Isolation Forest	[13]
Local Outlier Factor (LOF)	[14]
HBOS	[15]
COPOD	[16]
PCA baseline	(standard linear subspace baseline)
USAD	[17]
TranAD	[18]
OmniAnomaly	[8]
GDN	[19]
TimesNet	[20]

where the model-fitting phase is computationally expensive. For instance, at the CPU-1T tier, the ratio of inference to total throughput for OmniAnomaly reaches approximately $23\times$ on SMD and $55\times$ on Telemetry (see Table V). We define inference time as:

$$t_{\text{inf}} := \begin{cases} \tilde{t}_{\text{inf}}, & \text{if scoring-only time is instrumented,} \\ t_{e2e}, & \text{otherwise.} \end{cases} \quad (6)$$

The inference-time source is logged per run to make the comparison basis explicit.

b) Feasibility and throughput: Let N denote the number of scored units: for windowed methods $N = T - w + 1$ with series length T and window length w ; for non-windowed methods $N = T$. Throughput is $\text{wps} = N/t_{\text{inf}}$ in windows/ s . An entity is *feasible* at target τ if $\text{wps} \geq \tau$. We use $\tau = 500$ wps as a reference operating point corresponding to scoring at 500 Hz (2 ms period) under unit-stride windowing, i.e., one score per incoming sample. If τ is unmet, buffering or scoring latency grows without bound under sustained streaming. For windowed methods, w is taken from the method configuration, whereas for non-windowed methods $w = 1$ so $N = T$. Window scores are aligned to the window end timestamp for label comparison.

H. Throughput-Constrained Analysis

For each (method, dataset, τ), achievable performance under τ is the best AUC-PR among configurations whose measured throughput satisfies $\text{wps} \geq \tau$. Coverage at τ is the fraction of entities for which at least one configuration meets the target. This definition uses only measured runs (no extrapolation). Window-length scaling is frozen to the GPU-tier value for each method, so that scored-unit counts N are held constant across τ targets and throughput variation reflects only timing differences, not changes in N .

IV. EXPERIMENTAL SETUP

We benchmark a compact set of representative detector families (classical, deep, attention-based, graph-based). Table III lists evaluated methods and references. Classical baselines reflect common practice (often via PyOD [11]). Deep methods follow their original training and scoring procedures. Tier differences are induced solely by ECoLAD’s ladder and thread caps. Transformer-based methods rely on attention mechanisms [12].

Inputs are numeric feature vectors per timestamp. Detectors are trained unsupervised or self-supervised as defined by each method. Labels are used only for evaluation and feasibility statistics. RQ1 and the primary tier-wise analysis are reported on the proprietary telemetry dataset (Sec. III-B). RQ2 adds SMD to test whether degradation patterns transfer to a different domain and anomaly structure. RQ3 feasibility analysis is evaluated on telemetry, SMD, and SMAP to avoid overfitting conclusions to a single dataset. We report AUC-PR as the primary metric due to class imbalance and operational relevance.

V. RESULTS

A. RQ1: Cross-Tier Detection Quality

Table IV summarizes AUC-PR and normalized runtime across tiers for Telemetry and SMD. Overall, AUC-PR is not strictly invariant across tiers, but the magnitude of drift is strongly method- and domain-dependent.

a) *SMD*: OmniAnomaly stays near 0.51 AUC-PR across all tiers, USAD remains around 0.47–0.48, and PCA is essentially constant (0.448). In contrast, LOF degrades markedly under constrained tiers (0.145 on the reference tier down to 0.073 on CPU-1T). Several neural baselines (GDN, TimesNet) exhibit modest drift that can change relative ordering even when absolute changes are small.

b) *Telemetry*: Absolute AUC-PR values are low for most methods relative to SMD, and the ranking differs. The random-scorer baseline is 0.022 (anomaly rate $\pi = 0.02184$). HBOS achieves the highest AUC-PR (0.064 on the reference tier; 0.055 on CPU-1T), corresponding to approximately 2.9 \times lift above the random baseline. Several deep methods (USAD, TranAD, OmniAnomaly) cluster near 0.041 ($\approx 1.9\times$ above random) with minimal tier-to-tier change, indicating that compute reduction does not destabilize detection quality but that these methods offer limited separability on this signal. The low absolute values reflect the difficulty of aligning statistical novelty scores to event-log-derived fault labels in multivariate powertrain telemetry, not a scorer malfunction.

A single-tier accuracy leaderboard under-specifies deployment behavior: top methods on SMD differ from those on Telemetry, and tier-sensitive methods (e.g., LOF) shift substantially under constrained execution.

c) *Runtime regimes*: HBOS and COPOD occupy an ultra-low-cost regime (≈ 0.001 – 0.005 s/1k) across all tiers. IForest and PCA are substantially more expensive (up to ≈ 0.2 – 0.9 s/1k) despite being classical methods. Among neural methods, USAD scales smoothly with the ladder (0.021 \rightarrow 0.012 s/1k), whereas OmniAnomaly benefits strongly from compute reduction (0.213 \rightarrow 0.030 s/1k). TimesNet exhibits pronounced backend sensitivity: fast on GPU (0.095 s/1k) but substantially slower on CPU tiers (0.626–0.838 s/1k), indicating that hardware choice can dominate practical feasibility independently of accuracy.

B. RQ2: Degradation Modes and Bottlenecks

Fig. 2 separates quality drift (Panels A, C) from throughput collapse (Panel B). Three distinct degradation modes are

evident in Table V.

Backend/overhead-limited. TimesNet’s AUC-PR changes are modest across tiers, yet its CPU-tier cost rises sharply: inference wps on SMD drops from 9,569 at the GPU tier to 1,483 at CPU-1T, and on Telemetry from 11,164 to 1,751. Feasibility loss is therefore throughput-driven rather than accuracy-driven, and is masked when throughput results are pooled across tiers and datasets.

Quality-drift-limited. LOF maintains very high throughput across all tiers — exceeding 76,000 wps on Telemetry and 193,000 wps (median) on SMD at CPU-1T — but shows large negative Δ AUC-PR under tier scaling (Fig. 2C), indicating sensitivity to capacity reduction rather than a runtime bottleneck.

Graceful degraders. HBOS and COPOD retain high throughput and near-flat AUC-PR across all tiers, making them robust choices when predictable latency is the primary constraint. For HBOS, compute reduction actually increases throughput on Telemetry (from 70,503 wps at GPU to over 2,000,000 at CPU-1T) because the reduced work scale ($s = 0.25$) yields fewer histogram bins per scoring call. This effect is more modest on SMD where entity-level wps is already high.

The inference/full-run wps ratio is $1.0\times$ for all five classical methods (no per-entity fitting at scoring time). For neural methods the gap varies: OmniAnomaly’s per-entity fitting yields approximately 23 \times on SMD and 55 \times on Telemetry at CPU-1T. USAD and TranAD show more moderate gaps ($\approx 2\times$ and $\approx 2.5\times$ on SMD at CPU-1T, respectively). Reporting only full-run throughput for these methods would substantially understate their online scoring capacity.

C. RQ3: Throughput-Constrained Behavior on CPU-1T

a) *Coverage vs. throughput targets*: Fig. 1 shows that classical baselines retain high coverage over a wide τ range, while several deep models become infeasible at higher targets. Methods with CPU-1T inference wps well above the $\tau = 500$ wps CAN reference point (e.g., HBOS, COPOD, LOF) sustain coverage even at elevated targets, whereas methods near or below the reference (IForest at 4,199 wps; PCA at 1,752 wps; TimesNet at 1,483 wps on SMD) exhaust feasible configurations quickly as τ rises.

b) *Achievable AUC-PR under constraints*: Fig. 3 shows that as τ increases, feasible operating points shift toward lower-capacity configurations and detection quality can decrease. HBOS sustains 0.042 AUC-PR even at the highest feasible τ , while methods that become infeasible early provide no operating point above the random baseline at high throughput targets.

VI. DISCUSSION

ECoLAD formalizes compute reduction, thread caps, and throughput feasibility as explicit evaluation protocol variables. Our results suggest that rank drift under constrained execution is often driven by architectural throughput bottlenecks rather than accuracy degradation alone. This motivates a *feasibility-first* filtering approach, where detectors are first screened for

TABLE IV: SMD and Telemetry side-by-side AUC-PR and time/1k (means; time uses t_{inf} as defined in Sec. III-G). The Telemetry random-scoring baseline is AUC-PR = 0.022 (equal to the anomaly rate π); SMD anomaly rates vary by machine and a single baseline is not reported.

Model	SMD								Telemetry							
	AUC-PR \uparrow				time/1k \downarrow				AUC-PR \uparrow				time/1k \downarrow			
	GPU	CPU-MT	CPU-LT	CPU-1T	GPU	CPU-MT	CPU-LT	CPU-1T	GPU	CPU-MT	CPU-LT	CPU-1T	GPU	CPU-MT	CPU-LT	CPU-1T
<i>Random baseline (Telemetry): AUC-PR = 0.022</i>																
COPOD	0.250	0.250	0.250	0.250	0.005	0.005	0.005	0.005	0.035	0.035	0.035	0.035	0.002	0.002	0.002	0.002
GDN	0.296	0.302	0.272	0.307	0.073	0.070	0.046	0.033	0.051	0.048	0.050	0.049	0.053	0.043	0.029	0.018
HBOS	0.303	0.303	0.302	0.298	0.001	0.001	0.001	0.001	0.064	0.062	0.062	0.055	0.007	0.001	0.001	0.008
IForest	0.318	0.317	0.302	0.274	0.956	0.716	0.459	0.242	0.041	0.042	0.041	0.043	0.429	0.327	0.217	0.113
LOF	0.145	0.091	0.120	0.073	0.007	0.006	0.006	0.043	0.055	0.050	0.052	0.049	0.016	0.016	0.015	0.124
OmniAnomaly	0.504	0.511	0.512	0.511	0.213	0.141	0.082	0.030	0.041	0.041	0.041	0.041	0.210	0.140	0.081	0.028
PCA	0.448	0.448	0.448	0.448	0.577	0.573	0.578	0.601	0.037	0.037	0.037	0.037	0.132	0.132	0.134	0.136
TimesNet	0.280	0.292	0.282	0.312	0.095	0.840	0.657	0.337	0.057	0.051	0.055	0.050	0.082	0.792	0.626	0.317
TranAD	0.360	0.363	0.359	0.363	0.037	0.043	0.030	0.036	0.041	0.041	0.041	0.041	0.036	0.032	0.023	0.021
USAD	0.469	0.480	0.476	0.483	0.021	0.017	0.014	0.012	0.041	0.041	0.041	0.041	0.019	0.013	0.011	0.007

TABLE V: Inference throughput (wps, N/t_{inf}) across compute tiers, reported separately for SMD (22 entities; median with p10/p90 at CPU-1T) and Telemetry (single entity). Full-run wps (N/t_{e2e}) at CPU-1T exposes fit-overhead gaps; for classical methods the two are identical. The large inference/full-run gap for OmniAnomaly reflects per-entity model fitting: $\approx 23\times$ on SMD and $\approx 55\times$ on Telemetry at CPU-1T.

Model	SMD (22 entities)							Telemetry (1 entity)				
	Inference wps (median)				CPU-1T infer.		CPU-1T	Inference wps				CPU-1T
	GPU	CPU-MT	CPU-LT	CPU-1T	p10	p90	full-run	GPU	CPU-MT	CPU-LT	CPU-1T	full-run
COPOD	209 143	210 306	211 106	209 288	204 604	223 230	209 288	380 481	470 770	488 122	485 549	485 549
GDN	13 430	14 335	21 634	28 693	28 348	29 227	7527	18 309	23 295	34 172	50 583	2955
HBOS	721 912	765 987	830 247	913 376	884 285	945 698	913 376	70 503	1 686 248	1 864 450	2 058 696	2 058 696
IForest	1042	1377	2174	4199	4133	4292	4199	2322	3001	4596	8015	8015
LOF	153 040	164 988	176 400	193 397	171 927	213 962	193 397	59 168	63 179	69 094	76 420	76 420
OmniAnomaly	4688	6342	9032	18 000	17 871	18 036	780	4801	6360	9201	19 148	347
PCA	1715	1715	1701	1752	1658	1817	1752	7397	7612	7637	7516	7516
TimesNet	9569	1049	1075	1483	1471	1707	1433	11 164	1151	1178	1751	1274
TranAD	24 464	22 807	27 745	14 973	14 871	15 058	5890	27 840	30 620	38 565	27 333	4051
USAD	47 208	58 033	62 887	51 091	50 780	51 429	24 455	53 956	76 938	88 520	85 785	13 427

Performance & throughput degradation across compute tiers (GPU \rightarrow CPU \rightarrow Half \rightarrow ECU)

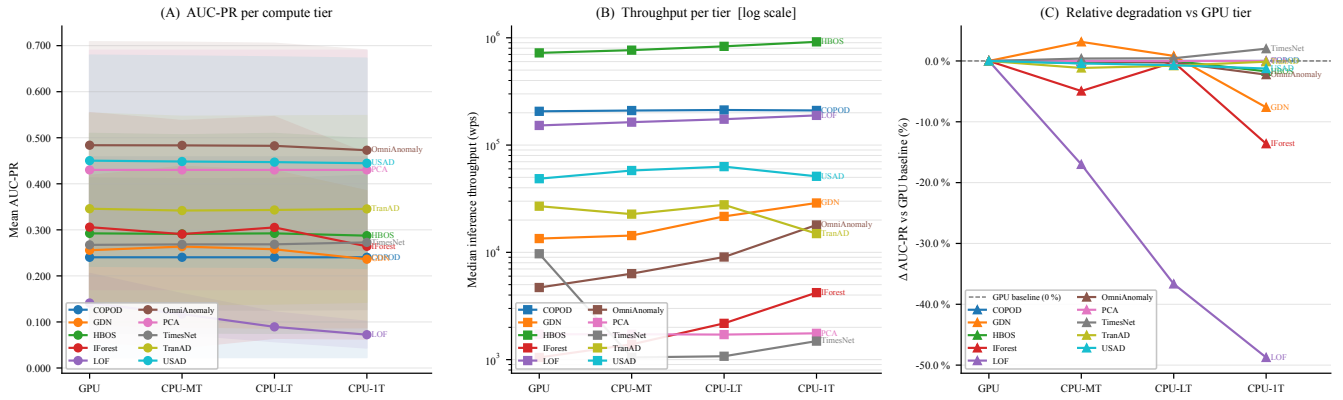


Fig. 2: Performance and throughput degradation across compute tiers (GPU \rightarrow CPU-MT \rightarrow CPU-LT \rightarrow CPU-1T). (A) Mean AUC-PR per method at each tier. (B) Median throughput (wps; log scale) from t_{inf} (Sec. III-G). (C) Relative AUC-PR change versus GPU tier (%).

deployment-relevant scoring rates before secondary metric-based selection.

While aggregate reporting provides a valuable global overview of algorithm performance, ECoLAD offers higher-resolution visibility into method-specific behaviors that vary by tier and dataset. For instance, backend-sensitive scaling in deep methods (e.g., TimesNet) or compute-driven throughput gains in histogram-based methods (e.g., HBOS) only become

apparent when throughput is disaggregated by execution tier. By fixing the semantics of scored units and window alignment, ECoLAD ensures cross-tier comparability and contributes a standardized framework for reporting detection quality alongside system costs.

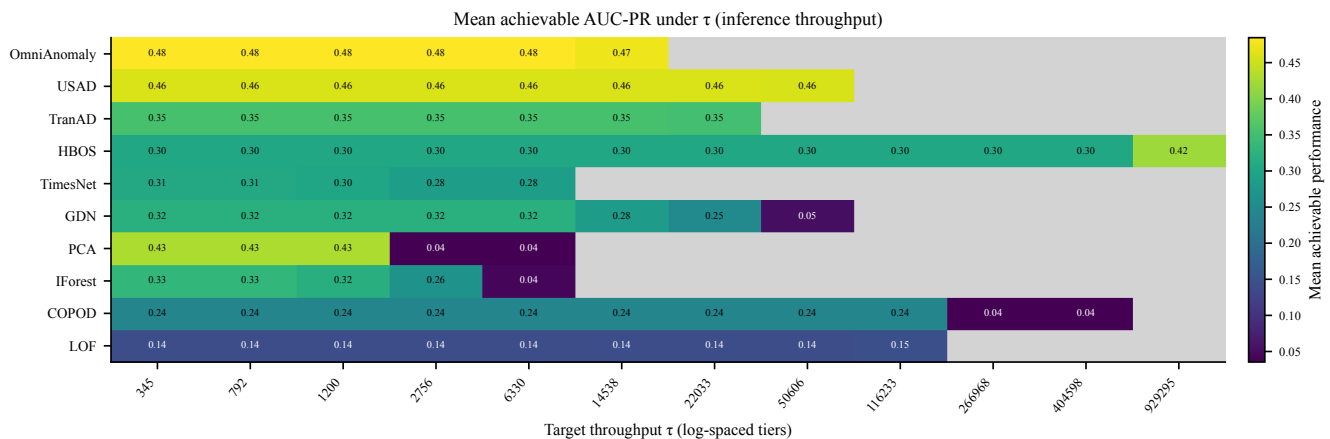


Fig. 3: Mean achievable detection quality under throughput targets on the constrained (CPU-1T) tier. Columns are throughput targets τ ; rows are methods. Each cell reports the mean AUC-PR achievable while meeting τ using t_{inf} (Sec. III-G). Hatched cells indicate targets where coverage falls below 50% of entities.

VII. LIMITATIONS

The telemetry dataset and pipeline code are proprietary and cannot be released due to industrial confidentiality constraints. However, the protocol is specified at a level of detail sufficient for independent re-implementation, as reflected by the \times Public entry in Table I.

While the CPU-1T tier isolates the effect of reduced parallelism, execution on an Apple M3 Max is not a cycle-accurate ECU emulation. We selected this SoC platform as it shares architectural characteristics, such as unified memory and heterogeneous CPU/GPU integration, with modern high-performance automotive compute platforms. Nevertheless, a platform-specific correction factor should be applied when mapping these throughput results to a specific target microarchitecture. Furthermore, the mechanical scaling rules provide a standardized baseline but may understate the best achievable performance possible through dedicated, per-tier hyperparameter retuning.

VIII. CONCLUSION

ECoLAD provides a deployment-oriented evaluation protocol for TSAD that makes compute reduction, CPU parallelism caps, throughput feasibility, and auditability explicit. Across automotive telemetry and public benchmarks, accuracy rankings shift under constrained execution, and throughput-feasible operating points can exclude otherwise competitive methods or require capacity reduction with measurable quality cost. Reporting throughput per tier and per dataset is necessary to expose backend-sensitivity and compute-reduction effects relevant to deployment decisions. ECoLAD complements accuracy-only leaderboards with a template for comparing detectors under deployment-relevant constraints.

REFERENCES

- [1] S. Schmidl, P. Wenig, and T. Papenbrock, "Anomaly detection in time series: A comprehensive evaluation," vol. 15, no. 9, pp. 1779–1797.
- [2] P. Wenig, S. Schmidl, and T. Papenbrock, "Timeeval: A benchmarking toolkit for time series anomaly detection algorithms," vol. 15, no. 12, pp. 3678–3681.
- [3] A. Zhang, S. Deng, D. Cui, Y. Yuan, and G. Wang, "An experimental evaluation of anomaly detection in time series," *Proc. VLDB Endow.*, vol. 17, no. 3, p. 483–496, Nov. 2023.
- [4] X. Qiu, Z. Li, W. Qiu, S. Hu, L. Zhou, X. Wu, Z. Li, C. Guo, A. Zhou, Z. Sheng, J. Hu, C. S. Jensen, and B. Yang, "Tab: Unified benchmarking of time series anomaly detection methods," 2025.
- [5] H. Si, J. Li, C. Pei, H. Cui, J. Yang, Y. Sun, S. Zhang, J. Li, H. Zhang, J. Han, D. Pei, and G. Xie, "Timeseriesbench: An industrial-grade benchmark for time series anomaly detection models," 2024.
- [6] A. Lavin and S. Ahmad, "Evaluating real-time anomaly detection algorithms – the numenta anomaly benchmark," in *2015 IEEE 14th International Conference on Machine Learning and Applications (ICMLA)*. IEEE, Dec. 2015, p. 38–44.
- [7] D. Choudhary, A. Kejariwal, and F. Orsini, "On the runtime-efficacy trade-off of anomaly detection techniques for real-time streaming data," 2017.
- [8] Y. Su, Y. Zhao, C. Niu, R. Liu, W. Sun, and D. Pei, "Robust Anomaly Detection for Multivariate Time Series through Stochastic Recurrent Neural Network," in *Proceedings of the 25th ACM SIGKDD International Conference on Knowledge Discovery & Data Mining*. Anchorage AK USA: ACM, Jul. 2019, pp. 2828–2837.
- [9] K. Hundman, V. Constantinou, C. Laporte, I. Colwell, and T. Soderstrom, "Detecting spacecraft anomalies using lstms and nonparametric dynamic thresholding," in *Proceedings of the 24th ACM SIGKDD International Conference on Knowledge Discovery & Data Mining*, ser. KDD '18. ACM, Jul. 2018, p. 387–395.
- [10] D. P. Kingma and J. Ba, "Adam: A Method for Stochastic Optimization," Jan. 2017, arXiv:1412.6980.
- [11] Y. Zhao, Z. Nasrullah, and Z. Li, "PyOD: A Python Toolbox for Scalable Outlier Detection," *Journal of Machine Learning Research*, vol. 20, no. 96, pp. 1–7, 2019.
- [12] A. Vaswani, N. Shazeer, N. Parmar, J. Uszkoreit, L. Jones, A. N. Gomez, L. Kaiser, and I. Polosukhin, "Attention is all you need," in *Proceedings of the 31st International Conference on Neural Information Processing Systems*, 2017, p. 6000–6010.
- [13] F. T. Liu, K. M. Ting, and Z.-H. Zhou, "Isolation Forest," in *2008 Eighth IEEE International Conference on Data Mining*, Dec. 2008, pp. 413–422, ISSN: 2374-8486.
- [14] M. M. Breunig, H.-P. Kriegel, R. T. Ng, and J. Sander, "LOF: identifying density-based local outliers," vol. 29, no. 2, pp. 93–104, 2000.
- [15] M. Goldstein and A. Dengel, "Histogram-based outlier score (hbos): A fast unsupervised anomaly detection algorithm," 09 2012.
- [16] Z. Li, Y. Zhao, N. Botta, C. Ionescu, and X. Hu, "COPOD: Copula-based outlier detection."
- [17] J. Audibert, P. Michiardi, F. Guyard, S. Marti, and M. A. Zuluaga, "USAD: UnSupervised anomaly detection on multivariate time series," in *Proceedings of the 26th ACM SIGKDD International Conference on Knowledge Discovery & Data Mining*. ACM, 2020, pp. 3395–3404.

- [18] S. Tuli, G. Casale, and N. R. Jennings, "TranAD: Deep Transformer Networks for Anomaly Detection in Multivariate Time Series Data," May 2022, arXiv:2201.07284.
- [19] A. Deng and B. Hooi, "Graph Neural Network-Based Anomaly Detection in Multivariate Time Series," Jun. 2021, arXiv:2106.06947.
- [20] H. Wu, T. Hu, Y. Liu, H. Zhou, J. Wang, and M. Long, "TimesNet: Temporal 2D-Variation Modeling for General Time Series Analysis," Apr. 2023, arXiv:2210.02186.